Clonally expanded novel multipotent stem cells from human bone marrow regenerate myocardium after myocardial infarction

Young-sup Yoon,[1] Andrea Wecker,[1] Lindsay Heyd,[1] Jong-Seon Park,[1] Tengiz Tkebuchava,[1] Kengo Kusano,[1] Allison Hanley,[1] Heather Scadova,[1] Gangjian Qin,[1] Dong-Hyun Cha,[2] Kirby L. Johnson,[2] Ryuichi Aikawa,[1] Takayuki Asahara,[1] and Douglas W. Losordo[1]

[1]Divisions of Cardiovascular Medicine and Cardiovascular Research, Caritas St. Elizabeth's Medical Center, and [2]Division of Genetics, Department of Pediatrics, Tufts-New England Medical Center, Tufts University School of Medicine, Boston, Massachusetts, USA.

We have identified a subpopulation of stem cells within adult human BM, isolated at the single-cell level, that self-renew without loss of multipotency for more than 140 population doublings and exhibit the capacity for differentiation into cells of all 3 germ layers. Based on surface marker expression, these clonally expanded human BM-derived multipotent stem cells (hBMSCs) do not appear to belong to any previously described BM-derived stem cell population. Intramyocardial transplantation of hBMSCs after myocardial infarction resulted in robust engraftment of transplanted cells, which exhibited colocalization with markers of cardiomyocyte (CMC), EC, and smooth muscle cell (SMC) identity, consistent with differentiation of hBMSCs into multiple lineages in vivo. Furthermore, upregulation of paracrine factors including angiogenic cytokines and antiapoptotic factors, and proliferation of host ECs and CMCs, were observed in the hBMSC-transplanted hearts. Coculture of hBMSCs with CMCs, ECs, or SMCs revealed that phenotypic changes of hBMSCs result from both differentiation and fusion. Collectively, the favorable effect of hBMSC transplantation after myocardial infarction appears to be due to augmentation of proliferation and preservation of host myocardial tissues as well as differentiation of hBMSCs for tissue regeneration and repair. To our knowledge, this is the first demonstration that a specific population of multipotent human BM-derived stem cells can induce both therapeutic neovascularization and endogenous and exogenous cardiomyogenesis.

Introduction

Congestive heart failure is a growing, worldwide epidemic (1). The major causes of heart failure are related to the irreversible damage that results from myocardial infarction (MI). Infarct size is a major determinant of morbidity and mortality, as large infarcts affecting 40% or more of the LV are typically associated with intractable cardiogenic shock or the rapid development of congestive heart failure (1, 2). The long-standing axiom has been that the myocardium has a limited capacity for self-repair or regeneration, and the irreversible loss of muscle, and accompanying contraction and fibrosis of myocardial scar, set into play a series of events, namely progressive ventricular remodeling of nonischemic myocardium, that ultimately leads to progressive heart failure (2). The loss of cardiomyocyte (CMC) survival cues is associated with diverse pathways for heart failure; this underscores the importance of maintaining the number of viable CMCs during heart failure progression. Currently, no medication or procedure used clinically, except for cardiac transplantation, has shown efficacy in replacing myocardial scar with functioning contractile tissue. Therefore, given the major morbidity and mortality associated with MI and heart failure, new approaches have been sought to address the principal pathophysiologic deficits responsible for these conditions, namely loss of vessels and CMCs. Recently, the identification of stem cells capable of contributing to tissue regeneration has ignited significant interest in the possibility that cell therapy could be used therapeutically for repair of damaged myocardium.

Previously, it was thought that tissue-specific stem cells could only differentiate into cells of the tissue of origin. Recently, however, a series of studies has suggested that adult tissue-specific stem cells may differentiate into lineages other than the tissue of origin, thus exhibiting plasticity in a process referred to as transdifferentiation. BM cells appear to have the capacity to repopulate many nonhematopoietic tissues, such as neuroectodermal cells (3, 4), skeletal myoblasts (5), CMCs (6, 7), endothelium (6–8), hepatocytes (9), and lung, gut, and skin epithelia (10). Recently, a subset of BM-derived stem cells referred to as multipotent adult progenitor cells (MAPCs) has been shown to proliferate extensively and differentiate into cells of all 3 germ layers (11). Thus, BM is regarded by many as a central repository for primitive stem cells that can repopulate somatic tissues. The extent of multilineage potential has been challenged, however, for example, in specific populations of HSCs (12, 13).

Therapeutic application of BM-derived stem cells has demonstrated that endothelial progenitor cells (14), angioblasts (15), or $CD34^+$ cells (16) transplanted into ischemic myocardium incorporate into foci of neovascularization and have a favorable impact on

Nonstandard abbreviations used: ANP, atrial natriuretic peptide; CFDA-SE, carboxyfluorescein diacetate succinimidyl ester; CMC, cardiomyocyte; cTnI, cardiac troponin I; DiI, CM-DiI; GalC, galactocerebroside; GFAP, glial fibrillar acidic protein; hBMSC, human BM-derived multipotent stem cell; IF, immunofluorescent; ILB4, isolectin B4; LVEDD, LV end-diastolic dimension; LVESD, LV end-systolic dimension; MAPC, multipotent adult progenitor cell; α-MHC, α-myosin heavy chain; MI, myocardial infarction; MSC, mesenchymal stem cell; NF200, neurofilament 200; NRCM, neonatal rat cardiomyocyte; pAb, polyclonal Ab; PD, population doubling; RAEC, rat aortic EC; RVSMC, rat VSMC; SMC, smooth muscle cell; TBMC, total BM cell; TRF, telomere restriction fragment; ULEX, Ulex europaeus agglutinin 1; WMSI, wall motion score index.

Conflict of interest: The authors have declared that no conflict of interest exists.

Citation for this article: *J. Clin. Invest.* **115**:326–338 (2005). doi:10.1172/JCI200522326.

cardiac function in the setting of myocardial ischemia. The more versatile potential of BM-derived HSCs has been documented with the use of side population cells (7) and the use of lineage-negative, *c-kit*–positive (Lin$^-$*c-kit*$^+$) cells (6); both kinds of cells differentiated into ECs, smooth muscle cells (SMCs), and CMCs in a murine MI model. These studies suggested the possibility that specific stem cell populations derived from murine BM could regenerate all the key elements of cardiac tissues and ameliorate ischemic cardiac dysfunction. Another source of adult stem cells being explored for possible cardiac regeneration is nonhematopoietic mesenchymal stem cells (MSCs; also called marrow stromal cells). MSCs can be derived from adult BM and have multilineage differentiation capacity (17, 18). The DNA-demethylating agent 5-azacytidine has been shown to induce multiple phenotypes, including CMCs (19). In animal models it has also been documented that human MSCs can undergo cardiomyogenic differentiation (20).

Although the above studies suggested that stem cells derived from BM have the potential to regenerate myocardial tissues, several questions remain with regard to their potential therapeutic use. Most importantly, it is yet unknown whether human adult stem cells have multipotency similar to that demonstrated in murine stem cells in terms of the multilineage differentiation required for cardiac regeneration. Currently, no human stem cells from BM have been shown to have the capacity to induce both therapeutic neovascularization and cardiomyogenesis in vivo, 2 of the key components for successful myocardial tissue regeneration. Studies with Lin$^-$*c-kit*$^+$ cells suggested similar potential; however, these studies were limited to mouse cells. Studies with side population cells (7) showed differentiation into multiple cellular types in vivo, but these studies were also performed with mouse cells and did not document any in vivo effects. Similarly, MAPCs were not tested for their in vivo effects on myocardial tissue repair. Another unanswered question is whether a single human stem cell is capable of participating in both neovascularization and myogenesis in myocardium. Thus far, the BM-derived cells, including endothelial progenitor cells, MSCs, side population cells, Lin$^-$*c-kit*$^+$ cells, and other HSCs used for cardiovascular regeneration, have consisted of heterogeneous populations of stem cells. Therefore, it is uncertain whether a single stem cell from BM can participate in both processes.

Here we have identified human BM-derived multipotent stem cells (hBMSCs) that are capable of expansion from a single cell, exhibit unlimited self-renewal, and are capable of triple-lineage differentiation into ECs, SMCs, and CMCs. The transplantation of hBMSCs into acutely infarcted myocardium attenuates cardiac dysfunction both by de novo differentiation of hBMSCs into myocardial tissues and by paracrine effects, which induced proliferation and preservation of host myocardial cells.

Results

Culture and characteristics of hBMSCs: clonality, surface epitopes, euploidy, and proliferation. We used 3 different marrow specimens from 3 different donors for stem cell cultures. After serial culture of total marrow cells in plastic dishes in DMEM with low (1 g) glucose containing 17% of FBS, cells were labeled with the red fluorescent dye CM-DiI (DiI). After limiting dilution (0.5 cell per well in a 96-well plate), we selected wells containing a single cell visualized by fluorescent microscopy. Cells in every well were monitored on a daily basis. Since cell proliferation did not commence for 48 hours, the daily monitoring provided at least a second opportunity to verify the presence of a single cell in each well. Of wells verified to contain a single cell (Figure 1A), 6% ± 4% (range 2–13%) demonstrated survival and proliferation of cells. When these cells were grown to 40–50% confluence, the cells from each well (representing the progeny of 1 clone) were reseeded into 1 well of 6-well plates and serially reseeded thereafter in 25-cm^2, 75-cm^2, and 175-cm^2 tissue culture flasks at a density of 4×10^3 to 8×10^3 cells per square centimeter. Subsequently, cells were cultured at a density of 4×10^3 to 8×10^3 cells per square centimeter in 175-cm^2 flasks and replated at 1:40 to 1:10 dilution. Reseeding was performed in triplicate, and the most rapidly growing clones were selected in every culture and expanded in serial culture. After more than 10 clones were obtained from each BM at passage 6, 2 clones were selected for continuous cultures. Morphologically, hBMSCs are less than 20 μm in diameter and exhibit a high nucleus-to-cytoplasm ratio (Figure 1B). Clonal cell lines derived in this manner have undergone more than 140 population doublings (PDs). Fluorescence-activated cell sorting (FACS; BD Biosciences) analysis using multiple surface epitopes demonstrated minimal expression (less than 3%) of CD90 (Thy1), CD105, and CD117 (c-kit) (Figure 1C). hBMSCs did not differentiate spontaneously and maintained their phenotype during culture expansion. In contrast, MSCs expressed high levels of CD29, CD44, CD73, CD105, CD90, and CD117 (Figure 1C). MHC class I (ABC) and class II (DR) molecules and known HSC markers (CD45, CD34, CD133, KDR, Tie2) were not expressed (see Supplemental Figure 1; supplemental material available online with this article; doi:10.1172/JCI200522326DS1). RT-PCR analysis was negative for Oct4 (data not shown), which is a known marker of ES cells and MAPCs (11). MAPCs are a clonal line of multipotent stem cells derived from adult mammalian BM that express CD13, SSEA1 (mouse) or SSEA3 (human), Flk-1, Thy1, and Sca1 (11, 21). These results indicated that hBMSCs do not belong to the previously described populations of BM-derived stem cells such as HSCs, MSCs, or MAPCs. Mean telomere restriction fragment (TRF) length of hBMSCs cultured for 5 PDs was 15.4 ± 0.3 kb; when retested after 120 PDs, mean TRF remained unchanged (15.2 ± 0.4 kb) (Figure 1D). Telomerase activity assessed by telomeric repeat amplification protocol (TRAP) assay was detected in hBMSCs with both low and high PDs (20 and 120 PDs, respectively; see Supplemental Figure 1C). DNA ploidy (the number of DNA copies) was examined by FACS analysis after staining of DNA with propidium iodide. hBMSCs cultured for 20 and 140 PDs from 3 different clones demonstrated no evidence for increased ploidy, suggesting that euploidy is maintained during culture expansion (Figure 1E).

Plasticity of hBMSCs: in vitro differentiation. We next tested the in vitro differentiation potential of hBMSCs by adopting and modifying previously published culture conditions for stem cells, which primarily require lineage-specific cytokines.

To induce differentiation into ECs, hBMSCs were replated at 5×10^4 cells per square centimeter in DMEM or EBM-2 with 2% FBS, 10^{-8} M dexamethasone, and 10 ng/ml VEGF, in glass chamber slides coated with either 0.1% gelatin or fibronectin. Five days after culture, hBMSCs formed vascular tubelike structures (Figure 2A, upper left panel). Fourteen days after culture, hBMSCs exhibited EC-specific phenotypes such as expression of vWFa, KDR, VE-cadherin, CD31, and the human-specific EC marker Ulex europaeus agglutinin 1 (ULEX) (Figure 2A). At 14 days, immunohistochemistry revealed EC markers VE-cadherin and ULEX were expressed in 63% ± 8% and 85% ± 12% of hBMSCs, respectively. RT-PCR for EC-specific genes VE-cadherin, CD34, KDR, Tie2, and CD31 also confirmed differentiation of hBMSCs into EC phenotypes (Figure 2B).

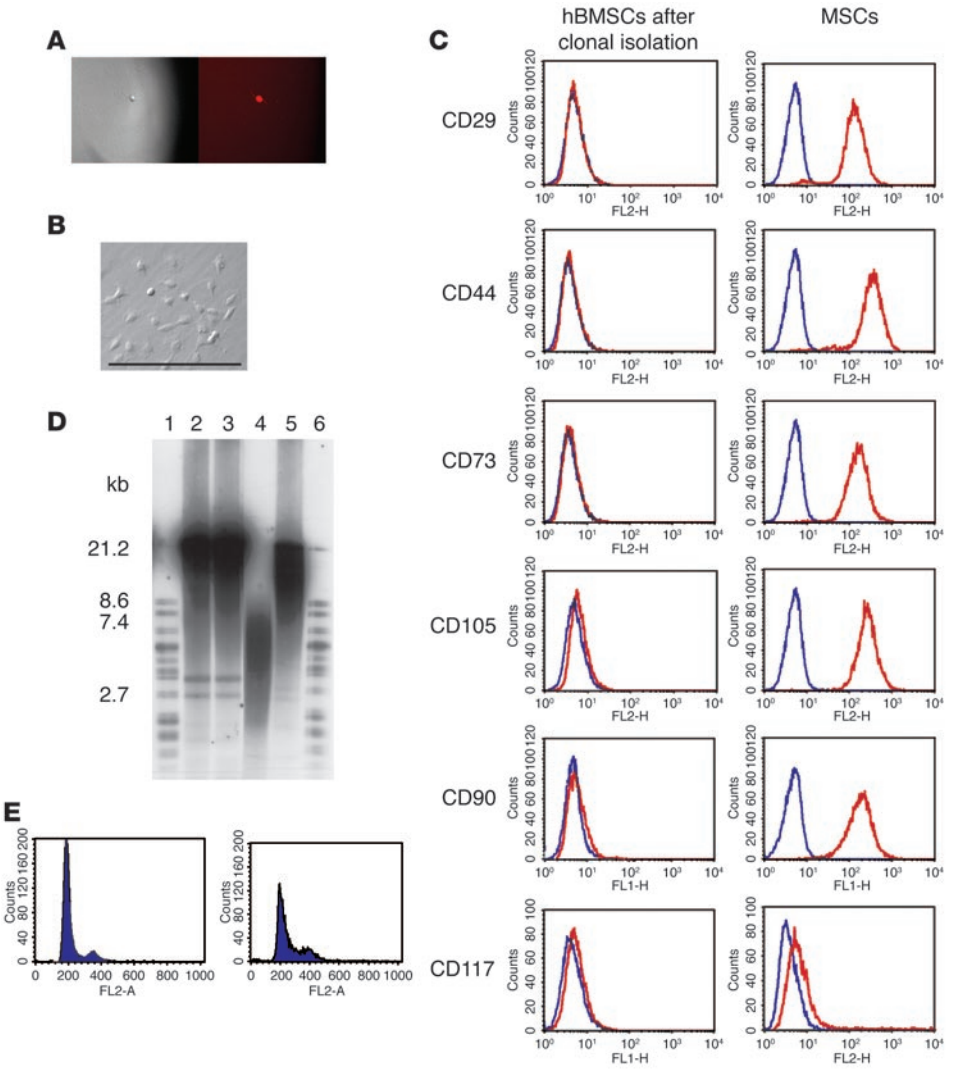

Figure 1
Characteristics of hBMSCs. (**A**) Phase-contrast and fluorescent images show a single cell per well. Original magnification, ×400. (**B**–**D**) Cells were analyzed with a FACStar flow cytometer. (**B**) Morphologically, most hBMSCs demonstrate round morphology with a cell size of less than 15 μm in diameter. Scale bar: 100 μm. (**C**) Clonally isolated hBMSCs cultured for 120 PDs were labeled with PE- or FITC-conjugated Abs against human CD29, CD44, CD73, CD105, CD90, or CD117, or Ig isotype controls. Blue lines, control Ig; red lines, specific Ab. Clonally isolated hBMSCs showed only minimal expression or no expression (<3%) of CD90, CD105, and CD117 (**C**). In contrast, the purchased MSCs expressed significantly higher levels of CD29, CD44, CD73, CD105, CD90, and CD117. (**D**) Mean TRF length of hBMSCs cultured for 5 PDs (lane 2) and 120 PDs (lane 3). No difference in mean TRF is shown. Human umbilical vein ECs (lane 4) and immortalized cell lines with high telomere length, provided by the Roche Diagnostics Corp. (lane 5), were used as controls. Lanes 1 and 6, molecular weight standards. (**E**) DNA ploidy analysis. hBMSCs were stained with propidium iodide and subjected to FACS analysis. Representative examples of hBMSCs cultured for 20 (left panel) and 140 (right panel) PDs demonstrate no evidence of overdiploid DNA content. Similar experiments were performed at least 3 times (**A**–**E**).

To induce differentiation into SMC lineages, hBMSCs were replated at 1×10^5 cells per square centimeter in noncoated or fibronectin-coated plastic dishes in 1–2% DMEM or EBM-2 supplemented with PDGF-BB (50 ng/ml) (22). Fourteen days after culture, 89% ± 6% and 67% ± 12% of hBMSCs stained positive for α-SMA and calponin, respectively, indicative of differentiation into SMC phenotypes (Figure 2C). RT-PCR confirmed the de novo expression of SMC-specific genes α-SMA, PDGFR-β, SM22α, and SM1 (Figure 2D).

To induce neural lineage differentiation, hBMSCs were plated at 4×10^4 per square centimeter on plastic dishes or poly-L-ornithine/laminin–coated dishes with 100 ng/ml bFGF, 20 ng/ml EGF, and B27 supplement in DMEM/F12 (3, 4). After 10–14 days, hBMSCs showed morphologic and phenotypic characteristics of various neural lineage cells (see Supplemental Figure 2, A–F). Immunofluorescent (IF) cytochemistry revealed expression of phenotypic markers of astrocytes (glial fibrillar acidic protein, GFAP), oligodendrocytes (galactocerebroside, GalC), and neurons (neurofilament 200, NF200; and β-tubulin III isoform) in 22% ± 7%, 15% ± 6%, and 57% ± 9% (for NF200) of hBMSCs, respectively. RT-PCR confirmed de novo expression of various neural lineage–specific genes such as GFAP, myelin basic protein (oligodendrocyte), microtubule-associated protein 2 (neuron), glutamic acid decarboxylase (neuron), and Tau (neuron).

We next tested whether hBMSCs could differentiate into endodermal lineages. hBMSCs were plated at 3×10^4 to 4×10^4 cells per square centimeter on 1% Matrigel in 2% FBS, supplemented with 10^{-8} M dexamethasone, 25 ng/ml HGF, 10 ng/ml FGF-4, and either 10 mg/ml DMSO or 0.5 mM sodium butyrate (21, 23). After 10–14 days of culture, approximately 60% of hBMSCs acquired epithelioid morphology. IF cytochemistry revealed expression of endodermal/hepatocytic genes HNF3β and αFP at day 10, and HNF1α and CK18 at day 14, in cultured hBMSCs (see Supplemental Figure 2, G–L). RT-PCR analysis revealed de novo expression of endodermal lineage–specific genes CK18, CK19, αFP, and albumin (see Supplemental Figure 2M).

Cardiomyogenic differentiation of hBMSCs after coculture with neonatal rat cardiomyocytes. To induce cardiomyogenic differentiation, hBMSCs were cocultured with neonatal rat cardiomyocytes (NRCMs). NRCMs were plated at 2×10^5 cells per square centimeter and cultured in DMEM (low glucose) containing 10% FCS. On day 3, hBMSCs labeled with DiI were added to the cultured NRCMs at a 1:4 ratio and cultured for up to 2 weeks. After fixation and staining

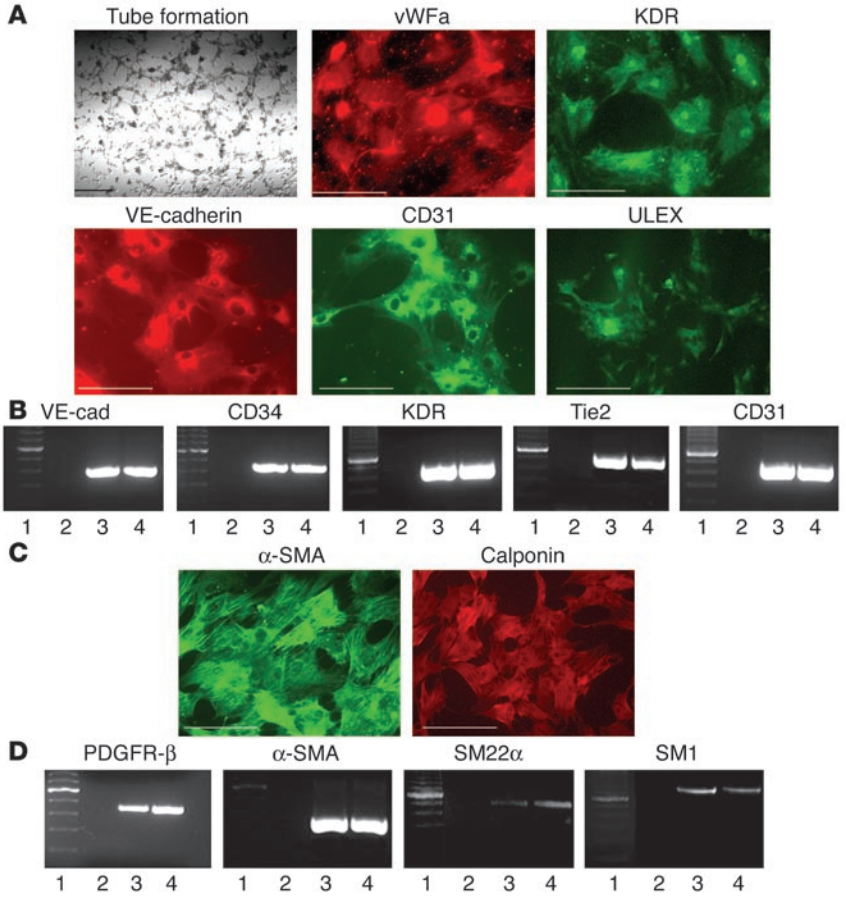

Figure 2

In vitro differentiation of hBMSCs into EC and SMC lineages. (**A**) Hoffman phase-contrast image (upper left panel) 5 days after culture with DMEM in gelatin-coated glass chambers shows that hBMSCs have formed typical vascular tubelike structures. Immunofluorescent imaging demonstrates that hBMSCs express EC-specific proteins such as vWFa, KDR, VE-cadherin, CD31, and ULEX after culturing in EC differentiation media for 14 days. (**B**) RT-PCR analysis using EC-specific primers VE-cadherin, CD34, KDR, Tie2, and CD31 also confirms the differentiation of hBMSCs into EC phenotypes. Lane 1, size marker; lane 2, before differentiation; lane 3, induced differentiation; lane 4, positive control. (**C**) hBMSCs cultured in 2% DMEM containing PDGF-BB for 14 days demonstrate the expression of SMC-specific proteins α-SMA and calponin by immunofluorescent staining. (**D**) RT-PCR analysis shows that SMC-specific genes PDGFR-β, α-SMA, SM22α, and SM1 are only expressed after induction of differentiation. Lane 1, size marker; lane 2, before differentiation; lane 3, induced differentiation; lane 4, positive control. The heavy band in the lanes of the size markers in **B** and **D** represents 600 bp. Scale bar: 100 μm.

with Abs against cardiac-specific proteins, IF images were obtained. DiI-labeled hBMSCs (Figure 3, B, F, and J) exhibit red fluorescence from the DiI label, and cells positive for CMC-specific proteins, such as cardiac troponin I (cTnI), atrial natriuretic peptide (ANP), and α-myosin heavy chain (α-MHC), appear green (Figure 3, C, G, and K). The merged images illustrate that a fraction of DiI-labeled hBMSCs also stained positive for the CMC-specific proteins, indicating that a subpopulation of hBMSCs were displaying features of CMC phenotype in coculture (Figure 3, D, H, and L). mRNA expression of cardiac transcription factors was evaluated by RT-PCR (Figure 3M). Before coculture, GATA-4 and Nkx2.5 were not expressed in hBMSC (lane 1) or in NRCM (lane 2) cultures. Coculture (lane 3) of hBMSCs and NRCMs induced de novo expression of GATA-4 and Nkx2.5. GATA-4 is a cardiac transcription factor that is known to activate the promoters of several cardiac genes, such as myosin light chain, troponin T, troponin I, α-MHC, and ANP. Nkx2.5 is one of the initial transcription factors involved in CMC differentiation (24). These findings suggest that hBMSCs have entered a differentiation pathway toward CMC phenotype. Of note, CMC differentiation of hBMSCs was not observed when hBMSCs were cocultured with conditioned medium from NRCMs (data not shown).

Phenotypic changes of hBMSCs consist of both fusion and differentiation. Recent studies have reported that the phenotypic changes of stem cells may occur as a consequence of cell fusion (25–28). To determine whether this mechanism underlies hBMSC differentiation, we used carboxyfluorescein diacetate succinimidyl ester–labeled (CFDA-SE–labeled) NRCMs (green fluorescence) and DiI-labeled hBMSCs for coculture, since neither of these chemical dyes is transferred to adjacent cells. Seven days after coculture, cultured cells were fixed and stained with cTnI followed by AMCA-conjugated secondary Ab (blue fluorescence) (Figure 3P). To avoid overlap of cells, we selected areas of single-cell layers for imaging analysis. As shown in Figure 3, N–Q, certain DiI-labeled hBMSCs, marked by an arrow, were also positive for green (NRCM) and blue (cTnI) fluorescence, which suggests that cell fusion had occurred. A truly differentiated cell is illustrated by the presence of red and blue fluorescence but the absence of green fluorescence (Figure 3, O–Q, arrowheads). These results indicate that both differentiation and fusion occur in the same coculture conditions. After 5,000 cells per coculture were counted from 3 different experiments, the prevalence of differentiation and fusion was 3.2% ± 0.9% and 2.9% ± 1.1%, respectively. To determine the occurrence of fusion between hBMSCs and ECs or SMCs, rat aortic ECs (RAECs) or rat VSMCs (RVSMCs), respectively, were cocultured with hBMSCs. When the RAECs and RVSMCs reached 50–60% confluence, cells were labeled with CFDA-SE (green fluorescence). Two days later, DiI-labeled hBMSCs were added to culture plates of RAECs and RVSMCs at a 1:4 ratio and cultured for 7 days. Then, cultured cells were fixed and stained with VE-cadherin or α-SMA followed by AMCA-conjugated secondary Ab. Using the above criteria for fusion and true differentiation under fluorescent microscopy, the prevalence of fusion was 5.3% ± 1.1% for ECs and 7.4% ± 0.9% for SMCs, while the prevalence of differentiation was 3.4% ± 0.7% for ECs and 3.6% ± 0.5% for SMCs (Figure 3, R–Y). The coculture of hBMSCs lentivirally transfected with GFP and NRCMs, RVSMCs, or RAECs adenovirally transfected with LacZ revealed prevalence of fusion and differentiation that was similar to that in the experiments using

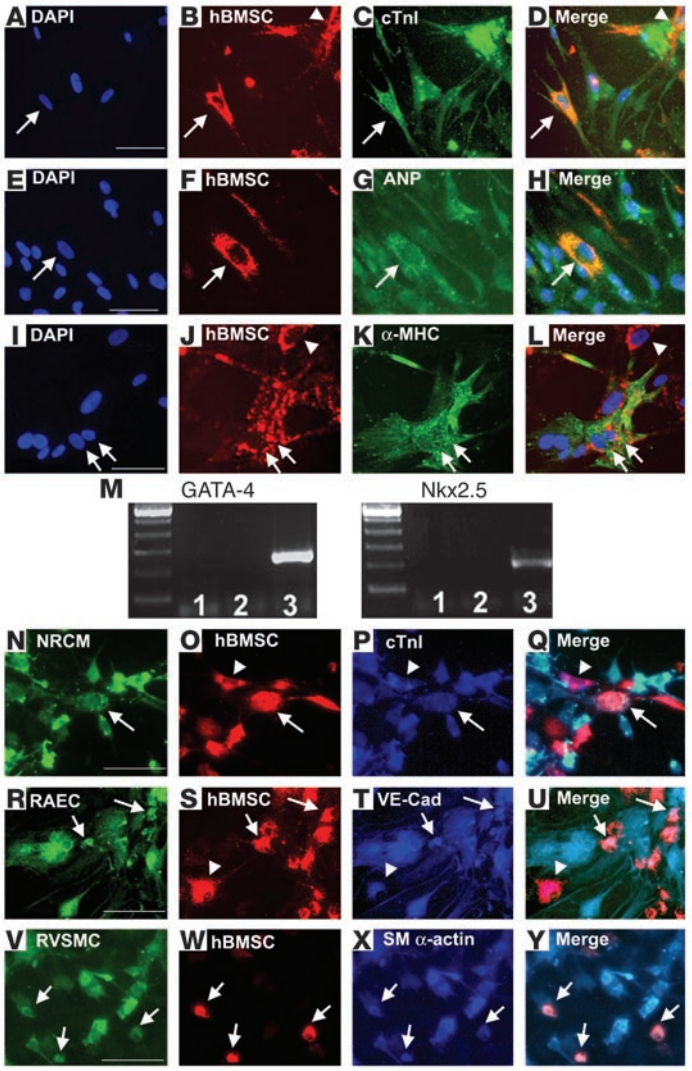

Figure 3
In vitro differentiation and fusion of hBMSCs to CMCs, ECs, and SMCs. (**A**–**L**) Coculture of hBMSCs with NRCMs. On day 3, DiI-labeled hBMSCs were added to the cultured NRCMs at a 1:4 ratio. IF images show cocultured DiI-labeled hBMSCs (**B**, **F**, and **J**) as red and NRCMs stained with CMC-specific proteins cTnI (**C**), ANP (**G**), and α-MHC (**K**) as green. Double-fluorescent cells in the merged images (**D**, **H**, and **L**) indicate that a subpopulation of hBMSCs exhibit CMC phenotypic markers (arrows). Arrowheads in **B**, **D**, **J**, and **L** indicate nontransdifferentiated hBMSCs. DAPI nuclear counterstaining (**A**, **E**, and **I**) shows no overlap of nuclei. mRNA expression of cardiac transcription factors was evaluated by RT-PCR (**M**). Before coculture, GATA-4 and Nkx2.5 were not expressed in hBMSC (lane 1) and NRCM (lane 2) cultures. Coculture (lane 3) induced de novo expression of GATA-4 and Nkx2.5. (**N**–**Q**) Coculture of prelabeled NRCMs and hBMSCs for investigation of cell fusion. NRCMs were labeled with the green fluorescence dye CFDA-SE (**N**) and DiI-labeled hBMSCs (**O**). Seven days after coculture, cells were stained for cTnI expression (blue fluorescence) (**P**). In the IF images (**N**–**Q**), triple-fluorescent cells (arrows) are fusion cells expressing cTnI protein. An hBMSC that has differentiated into CMC lineage is illustrated by red and blue fluorescence without green fluorescence (arrowheads). (**R**–**Y**) To determine the contribution of fusion and differentiation to phenotypic changes of hBMSCs into ECs (**R**–**U**) or SMCs (**V**–**Y**), CFDA-SE–labeled RAECs or RVSMCs were cocultured with DiI-labeled hBMSCs. Cells were stained with VE-cadherin or α-SMA (blue fluorescence). Arrows in **R**–**U** indicate fused RAECs (green) and hBMSCs (red) that express VE-cadherin. Arrowheads in **R**–**U** illustrate ECs differentiated from hBMSCs. Arrows in **V**–**Y** indicate fused RVSMCs (green) and hBMSCs (red) that express α-SMA. Scale bar in **A**–**L**: 50 μm; scale bar in **N**–**Y**: 100 μm.

chemical dyes (see Supplemental Figure 4). These results reveal that phenotypic changes of hBMSCs in coculture can result from both fusion and differentiation and suggest that caution must be used in the interpretation of immunohistochemistry using lineage-specific marker proteins to define differentiation of stem cells. Of course, the rates of fusion and differentiation in vivo may differ from those documented in vitro. In addition it should be noted that our observations are limited to a certain time frame, and it is currently not known whether the fused cells survive for significant periods of time.

hBMSC transplantation results in favorable remodeling and improves cardiac function after MI. The degree of stem cell plasticity observed in vitro prompted us to test whether ischemic or jeopardized myocardium could be protected or restored by transplantation of hBMSCs. Shortly after coronary ligation in nude rats, 8×10^5 hBMSCs were transplanted by direct injection into the ventricular wall of the peri-infarct area. The same number of human total BM cells (TBMCs) and the same volume of PBS were used as controls. Of 15 rats that underwent surgery, 14 rats receiving hBMSCs survived, whereas 12 rats survived in the TBMC and PBS groups, during the study period of 4 weeks.

To evaluate cardiac function, echocardiography was performed before and 3 days and 4 weeks after surgery. LV end-diastolic dimension (LVEDD), LV end-systolic dimension (LVESD), fractional shortening, and wall motion score index (WMSI) were similar among rats receiving hBMSCs, TBMCs, or PBS before and 3 days after surgery (Figure 4, A and B). Echocardiography performed 4 weeks after treatment revealed that both LVEDD and LVESD were significantly smaller (LVEDD, $P < 0.05$ vs. TBMC and PBS, respectively; LVESD, $P < 0.01$ vs. TBMC and PBS, respectively) (Figure 4, A and B), and thus fractional shortening was significantly greater ($P < 0.01$ vs. TBMC and PBS, respectively) (Figure 4C), in rats receiving hBMSCs than in those treated with TBMCs or PBS. WMSI, which represents the extent of regional wall motion abnormalities, was significantly better in the hBMSC-transplanted group ($P < 0.01$ vs. TBMC and PBS, respectively) (Figure 4D). LVEDD, LVESD, fractional shortening, and WMSI were not different between TBMC- and PBS-treated rats. Of note, the incidence of dyskinesia was 14% versus 58% and 67% in hBMSC-treated versus TBMC- and PBS-treated rats, respectively ($P < 0.05$). Invasive hemodynamic measurements demonstrated that LV systolic pressure, $+dP/dt_{max}$ (maximal rate of pressure rise), and $-dP/dt_{max}$ (maximal rate of pressure fall) were all

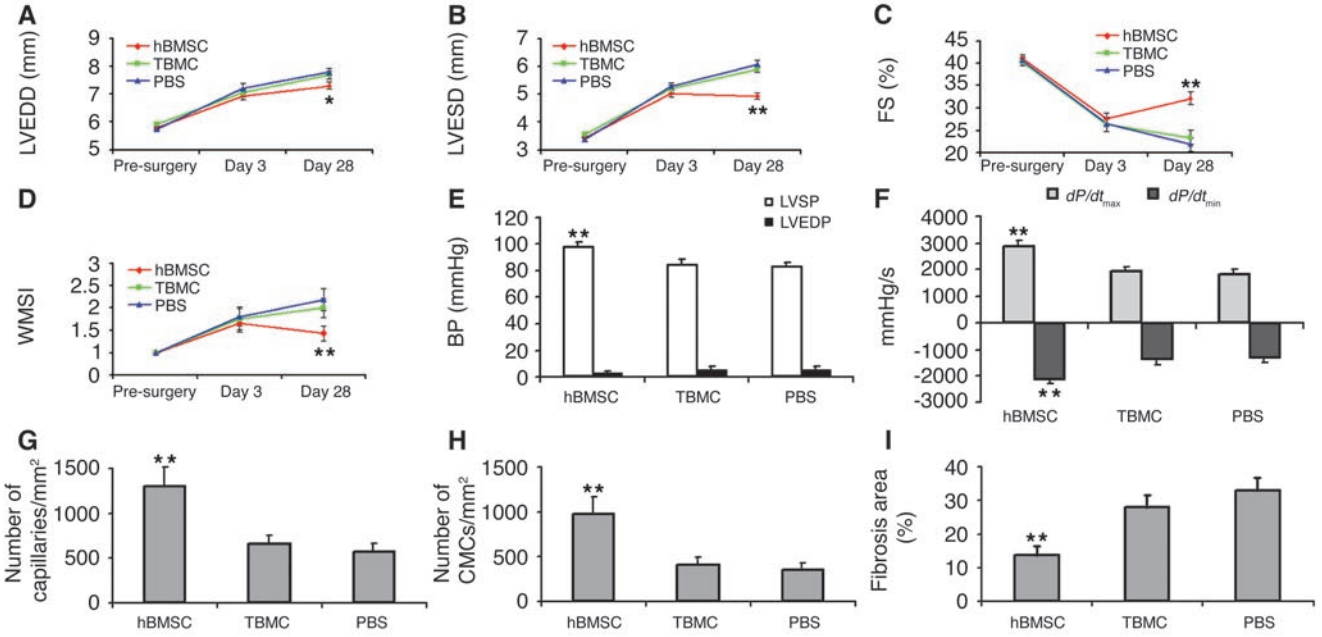

Figure 4

Transplantation of hBMSCs improves cardiac function, increases capillary and CMC density, and decreases myocardial fibrosis in a rat model of MI. (**A**–**D**) Echocardiographic parameters 4 weeks after MI and cell transplantation show smaller LVEDD and LVESD, better fractional shortening (FS), and lower WMSI in the hBMSC-transplanted rats than in the TBMC- and PBS-treated rats, indicating improved cardiac function. (**E** and **F**) Invasive hemodynamic measurements using a Millar Instruments Inc. catheter 4 weeks after hBMSC transplantation. LV systolic pressure (LVSP) (**E**) and $+dP/dt_{max}$ and $-dP/dt_{max}$ (dP/dt_{min}) (**F**) were significantly augmented in the hBMSC-transplanted rats compared with the control groups. LVEDP, LV end-diastolic pressure. $^{*}P < 0.05$, $^{**}P < 0.01$. (**G** and **H**) Capillary (**G**) and CMC (**H**) density measured after CD31 and H&E staining, respectively, was significantly higher in hBMSC-transplanted hearts than in TBMC- and PBS-treated hearts. $^{**}P < 0.01$ vs. TBMC and PBS. (**I**) Percentage circumferential fibrosis measured in Masson's trichrome–stained sections was significantly smaller in hBMSC-transplanted hearts. $^{**}P < 0.01$ vs. TBMC and PBS.

significantly greater (i.e., indicative of better LV performance) in the hBMSC-transplanted rats than in the TBMC- or PBS-injected rats (all $P < 0.01$, respectively) (Figure 4, E and F). Together, these data indicate that hBMSC transplantation results in enhanced functional recovery and more favorable remodeling after MI.

Transplantation of hBMSCs increases capillary and CMC density and decreases myocardial fibrosis. To determine the impact of hBMSC transplantation on the pathologic features of infarcted myocardium, capillary and CMC density was quantified after CD31 and H&E staining, respectively, and the percentage circumferential fibrosis area was measured. Capillary density was 2- and 2.3-fold higher in the hBMSC-transplanted rats than in the TBMC- and PBS-injected rats, respectively ($P < 0.01$) (Figure 4G; see Supplemental Figure 3A). CMC density was also 2.4- and 2.8-fold higher in the hBMSC-transplanted rats than in the TBMC- and PBS-injected rats, respectively ($P < 0.01$) (Figure 4H; see Supplemental Figure 3B). Percentage circumferential fibrosis area measured in Masson's trichrome–stained sections demonstrated a smaller area of fibrosis in the hBMSC-transplanted hearts ($P < 0.01$ vs. TBMC, PBS) (Figure 4I; see Supplemental Figure 3C, blue-colored area).

Engraftment and multilineage differentiation of transplanted hBMSCs in vivo: evidence for vasculogenesis and exogenous cardiomyogenesis. To determine the extent and magnitude of transplanted hBMSC engraftment, myocardial sections from frozen samples were examined 4 weeks after transplantation. Under fluorescent microscopy, we observed engraftment of numerous DiI-labeled hBMSCs in the peri-infarct and infarct region (Figure 5, A and B). In contrast, the TBMC-transplanted heart showed smaller numbers of scattered DiI-labeled cells, which were mostly located within the infarct region (Figure 5, C and D). Immunophenotypic characterization revealed that engrafted DiI-labeled hBMSCs (red) were stained positive for CMC-specific proteins cTnI and ANP (green) (α-MHC data not shown) and formed a mass of CMCs that appeared morphologically mature and were indistinguishable from host CMCs in the peri-infarct and infarct area (Figure 5, E and F); this suggests CMC differentiation. Phenotypic changes of hBMSCs into ECs and SMCs were also confirmed by the colocalization of transplanted hBMSCs with isolectin B4–positive (ILB4-positive) vascular ECs and α-SMA–positive SMCs, which suggests differentiation into EC (Figure 5, G and H) and SMC (Figure 5I) phenotypes. We detected CMC differentiation only in hBMSC-transplanted rats. Differentiation into CMCs, defined by morphologic similarity and CMC-specific protein expression (cTnI), was observed in 12 of 14 surviving hBMSC-transplanted rats (85%). An organized mass of regenerating CMCs similar to normal host myocardium as seen in Figure 5, H and I, and Figure 6C was found in 9 of 14 rats (64%), and only scattered cellular differentiation was observed in 3 other rats (21%). However, CMC-specific protein expression in transplanted hBMSCs was observed in all hBMSC-transplanted rats. EC and SMC differentiation defined by morphology and marker positivity was found in all hBMSC-transplanted rats examined. In the peri-infarct zone the prevalence of transdifferentiated CMCs was 4.1% ± 3.1%, that of capillaries including transdifferentiated ECs was 5.4% ± 3.3%, and that of arteries or arterioles containing transdifferentiated SMCs was 5.8% ± 2.9%.

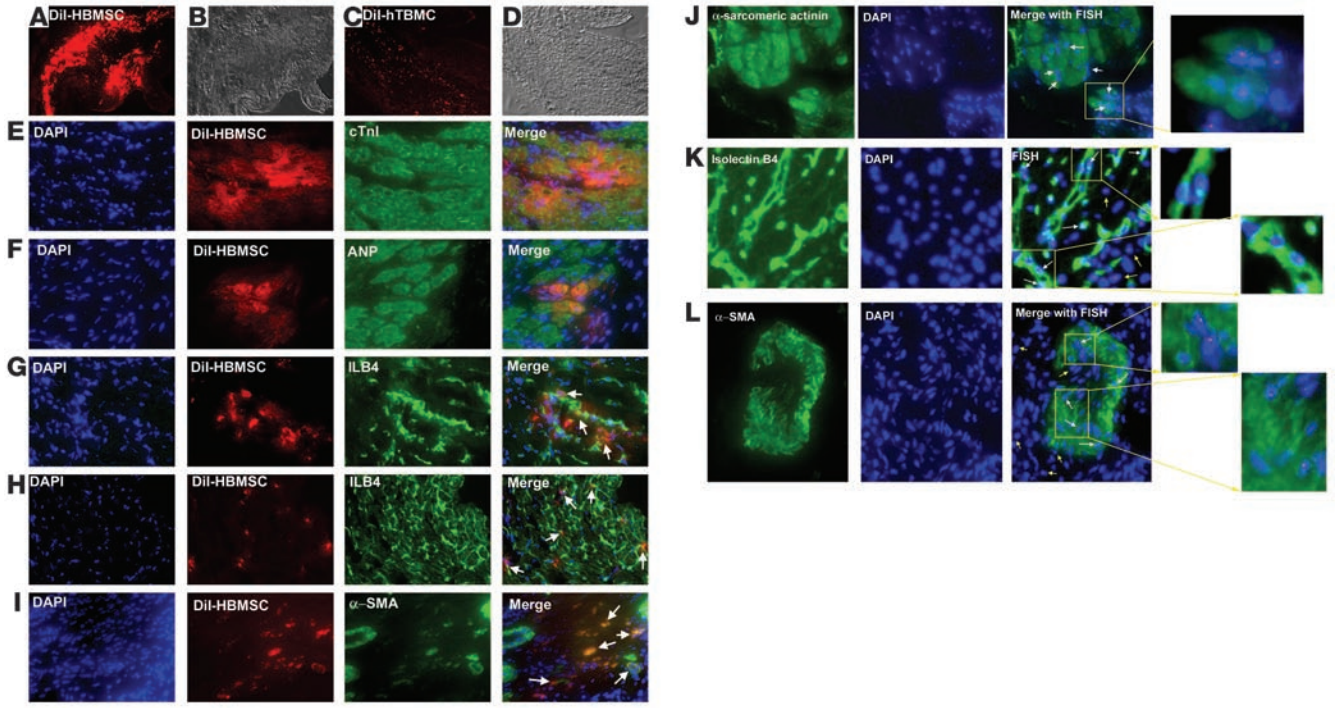

Figure 5
Engraftment and multilineage differentiation of transplanted hBMSCs in infarcted myocardium. (**A**–**D**) Engraftment of DiI-labeled hBMSCs and TBMCs into infarcted myocardium. Numerous hBMSCs (red fluorescence) (**A**) are engrafted into the infarct and peri-infarct region of myocardium at 4 weeks after transplantation. In contrast, considerably fewer TBMCs (red fluorescence) are observed, mostly within the infarct area (**C**). **B** and **D** are the Hoffman images of **A** and **C**, respectively, showing the localization of engrafted cells. (**E** and **F**) Immunophenotypic characterization of hBMSCs that have differentiated into CMCs. Myocardial samples 4 weeks after transplantation were stained for cTnI (**E**) and ANP (**F**) (each detected with FITC-labeled secondary Ab). Transplanted DiI-hBMSCs expressed both markers and were indistinguishable from host CMCs. (**G** and **H**) Myocardial sections stained with ILB4, an EC marker, demonstrate that DiI-hBMSCs are colocalized with vascular ECs in both the infarct (**G**) and the peri-infarct (**H**) area (arrows). (**I**) Myocardial sections stained with α-SMA illustrate DiI-hBMSC colocalized with vascular SMCs (arrows). (**J**–**L**) FISH on hBMSC-transplanted hearts. FISH with α-sarcomeric actinin staining (**J**) demonstrates that transplanted hBMSCs shown in FISH-positive red fluorescence express a CMC phenotype (green fluorescence). FISH with ILB4 staining (**K**) demonstrates that transplanted hBMSCs shown in FISH-positive red fluorescence exhibit a vascular EC phenotype (green fluorescence). FISH with α-SMA staining (**L**) reveals that transplanted hBMSCs shown in FISH-positive red fluorescence express an SMC phenotype (green fluorescence). White arrows indicate FISH-positive cells stained with CMC, EC, or SMC markers; yellow arrows indicate FISH-positive cells not stained with CMC, EC, or SMC markers. Scale bars in **A**–**I**: 100 μm; scale bars in **J**–**L**: 50 μm.

To further confirm the differentiation into CMC, EC, and SMC lineages, we performed FISH followed by immunohistochemistry with lineage-specific Abs. Under fluorescent microscopy, multiple FISH signals were detected in CMCs, ECs, and SMCs, which suggested that the transplanted hBMSCs had differentiated into multiple lineages (Figure 5, J–L). Together, these findings suggested that transplanted hBMSCs were robustly engrafted in the infarct or ischemic myocardium, survived for prolonged periods of time, and resulted in de novo myogenesis and vasculogenesis. Of note, pathologic investigation revealed no teratoma, tumor, angiomatosis, or bone formation in hBMSC-transplanted hearts.

Transplanted hBMSCs augment proliferation and survival of host myocardium: evidence for angiogenesis and endogenous cardiomyogenesis. We also considered the possibility that some of the physiologic effect of hBMSC transplantation may not solely be explained by the extent of multilineage differentiation in situ. Accordingly, we next sought to elucidate whether transplanted hBMSCs affected proliferation and survival of host myocardial cells. To determine the proliferative fraction of host myocardial cells, we implanted miniosmotic pumps delivering BrdU constantly for 4 weeks to label all cells that entered the S phase of the cell cycle. In sections from hBMSC-transplanted hearts, numerous proliferating cells were observed in both host myocardial cells and transplanted cells (Figure 6, A–D). In contrast, considerably fewer BrdU-positive cells were observed in TBMC- or PBS-injected hearts (Figure 6, E and F). The BrdU index, the percentage of the BrdU-positive nuclei counted in each section, in the peri-infarct area was significantly higher in hBMSC-transplanted hearts than in controls (hBMSC vs. TBMC and PBS: 25.8% ± 5.2% vs. 11.2% ± 3.1% and 9.5% ± 2.8%, respectively, $P < 0.001$). Double-IF histochemistry using mAbs against BrdU and either cTnI or ILB4 revealed that both CMCs and ECs were positive for BrdU (Figure 6, G–N). The BrdU indices of ECs and CMCs were again higher in hBMSC-transplanted hearts (hBMSC vs. TBMC and PBS: ECs, 8.3 ± 2.7 vs. 2.9 ± 1.5 and 2.4 ± 1.3, respectively, $P < 0.01$; CMCs, 2.1 ± 1.2 vs. 0.2 ± 0.1 and 0.2 ± 0.1, respectively, $P < 0.01$). The total BrdU index in the normal portion of myocardium was also significantly higher in hBMSC-transplanted hearts (hBMSC vs. TBMC and PBS: 2.8 ± 0.3 vs. 1.4 ± 0.4 and 1.2 ± 0.4, respectively, $P < 0.05$). Furthermore, we performed Ki-67 staining to verify the proliferation of host myocardial cells. The Ki-67 index was also significantly higher

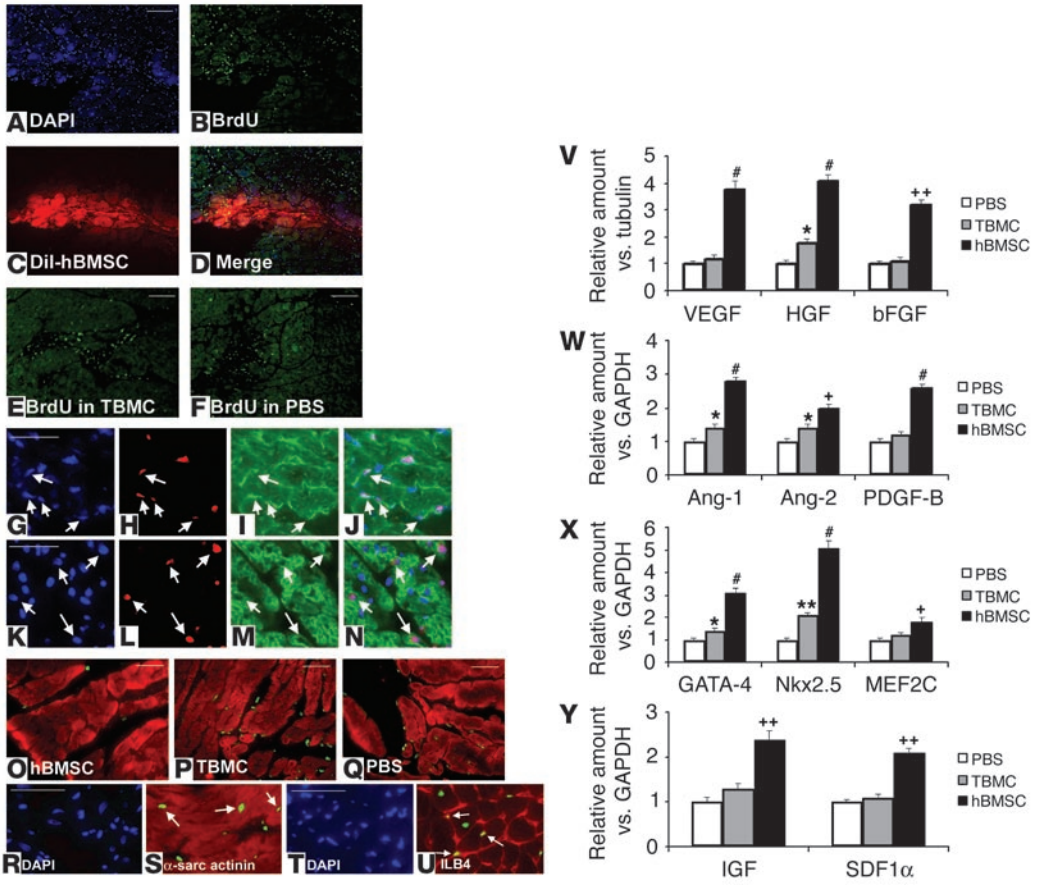

Figure 6

hBMSC transplantation augments myocardial cell proliferation, reduces myocardial apoptosis, and affects multiple paracrine factors. (**A**–**F**) BrdU imunohistochemistry. (**A**–**D**) Numerous BrdU-positive cells (green fluorescence) were observed in both host myocardial cells and transplanted cells in hBMSC-transplanted hearts (**D**), in contrast to TBMC-treated (**E**) or PBS-treated (**F**) hearts. (**G**–**J**) Double staining for BrdU (**H**) and ILB4 (**I**) shows proliferating capillary ECs (arrows). (**K**–**N**) Double staining for BrdU (**L**) and cTnI (**M**) shows proliferating cells (arrows) (**N**) in hBMSC-transplanted hearts. (**O**–**Q**) hBMSC-treated (**O**), TBMC-treated (**P**), or PBS-treated (**Q**) myocardium with anti–α-sarcomeric actinin mAb and TUNEL to identify apoptotic myocardial cells (green fluorescence). Fewer apoptotic cells are evident in hBMSC-transplanted hearts compared with those receiving TBMCs or PBS. (**R** and **S**) Staining with mAb against α-sarcomeric actinin (red) and TUNEL (green) demonstrates CMC apoptosis (arrows) in PBS-injected heart tissue. (**T** and **U**) Staining with ILB4 (red) and TUNEL (green) demonstrates EC apoptosis (arrows) in the PBS-injected heart. Scale bar: 100 μm (**A**–**F** and **O**–**U**), 50 μm (**G**–**N**). (**V**–**Y**) Heart samples (n = 3 per group) were harvested 4 weeks after MI and cell transplantation. Quantification of protein expression normalized to tubulin expression (**V**) demonstrates significant upregulation of VEGF, bFGF, and HGF in hBMSC-transplanted hearts compared with TBMC- or PBS-injected hearts. mRNA expression of angiogenic cytokines (**W**), cardiac transcription factors (**X**), and other factors (IGF and SDF1α) (**Y**) normalized to GAPDH expression shows significant upregulation of all factors in the hBMSC-transplanted hearts. Data were obtained from 3 separate experiments and are presented as amount relative to controls. $^{*}P < 0.05$, $^{**}P < 0.01$ vs. PBS; $^{+}P < 0.01$, $^{++}P < 0.001$, $^{\#}P < 0.0001$ vs. TBMC and PBS. Ang, angiopoietin.

in hBMSC-transplanted hearts (see Supplemental Figure 5). These results indicate that the transplanted hBMSCs augment proliferation of host myocardial cells including ECs and CMCs.

Next, we investigated whether transplanted cells could affect apoptosis, generally regarded as one of the main mechanisms responsible for ongoing myocardial degeneration after acute MI. TUNEL assays were performed using myocardial samples 1 week after transplantation. The apoptotic index, the percentage of TUNEL-positive nuclei, was significantly lower in hBMSC-transplanted hearts in the infarct area (apoptotic index vs. TBMC and PBS: 3.4 ± 0.8 vs. 6.5 ± 1.1 and 6.8 ± 0.9, respectively, $P < 0.05$) and the difference of apoptotic index was more prominent in the peri-infarct area (apoptotic index vs. TBMC and PBS: 2.1 ± 0.8 vs. 6.6 ± 1.2 and 7.3 ± 1.1, respectively, $P < 0.01$) (Figure 6, O–Q). These results were confirmed by activated caspase-3 staining, which also demonstrated a similar magnitude of decreased myocardial apoptosis in hBMSC-transplanted hearts (see Supplemental Figure 5). The apoptotic index of CMCs and ECs obtained after concomitant staining of α-sarcomeric actinin or ILB4 and TUNEL assay was significantly decreased in hBMSC-transplanted hearts (hBMSC vs. TBMC and PBS: CMCs, 0.5 ± 0.1 vs. 2.1 ± 0.3 and 1.9 ± 0.3, respectively, $P < 0.01$; ECs, 0.7 ± 0.1 vs. 2.5 ± 0.3 and 2.0 ± 0.2, respectively, $P < 0.01$) (Figure 6, R–U). Thus, an additional mechanism by which hBMSC transplantation can preserve myocardial function, promoting survival of endangered CMCs and ECs, is elucidated by these studies.

Paracrine effect of transplanted hBMSCs: upregulation of angiogenic cytokines and cardiac transcription factors. To identify potential paracrine mechanisms responsible for the therapeutic effect of

hBMSCs after myocardial injury, we evaluated protein or mRNA expression of multiple paracrine factors using cardiac samples 4 weeks after transplantation ($n = 3$ per group). Expression of certain angiogenic cytokines such as VEGF-A, HGF (29), bFGF, angiopoietin-1 and -2 (30), and PDGF-B (31) was significantly upregulated in the hBMSC-transplanted hearts compared with those receiving TBMCs or PBS ($P < 0.01$ and $P < 0.0001$, respectively; Figure 6, V and W). These findings suggest that transplanted hBMSCs can modulate expression of multiple angiogenic cytokines with the potential to promote angiogenesis as well as vasculogenesis. Cardiac transcription factors such as GATA-4, Nkx2.5, and MEF2C were also significantly upregulated in the hBMSC-transplanted hearts compared with the controls (Figure 6X), which suggests that transplanted hBMSCs could enhance myogenesis by augmenting host CMC proliferation and differentiation, and/or directly differentiating into new CMCs. Other factors significantly upregulated in the hBMSC-transplanted hearts included IGF-1, well known for its effects on myocardial tissue, including stimulation of cardiac contractility, antiapoptotic effects, and improved remodeling after MI; and stromal cell–derived factor-1α (32), which is a chemokine known to contribute to potent neovascularization by recruiting hematopoietic and endothelial progenitor cells (Figure 6Y). Collectively, the upregulation of multiple paracrine factors can, in part, explain the proliferative and protective effect of transplanted hBMSCs on host tissues including ECs and CMCs.

Discussion

A novel adult human stem cell population, hBMSCs, which appears distinct from previously described populations of adult stem cells, was clonally isolated, beginning at the single-cell level, from mixed total BM cell culture. Clonally isolated hBMSCs differentiated into cells of 3 germ layers (endoderm, mesoderm, and neuroectoderm) and self-renewed in culture for more than 140 PDs without obvious loss of plasticity or onset of replicative senescence. The transplantation of hBMSCs into a model of MI ameliorates the functional and pathologic changes following MI. The mechanism of improved cardiac function not only consists of differentiation of transplanted stem cells into essential myocardial tissues such as CMCs, ECs, and SMCs but also involves paracrine effects of the transplanted stem cells, which stimulate the proliferation of host myocardial tissues, including ECs and CMCs, and prevent apoptosis of endangered cells following ischemic injury.

The hBMSCs that we have identified are a unique population of adult BM-derived multipotent stem cells in that they express minimal levels (less than 3%) of CD90, CD105, and CD117. None of the characteristic marker panels defining HSCs, MSCs, and MAPCs matches the profile of hBMSCs. hBMSCs do not express the well-known MSC marker proteins CD29, CD44, and CD73 (also called SH3 or SH4) (33, 34). The minimal expression of surface molecules appears to be a prerequisite for the plasticity of hBMSCs as shown in other adult multipotent stem cells (11). In contrast to MAPCs, hBMSCs do not express genetic markers of ES cells, such as Oct4, which are believed to be essential for MAPC function. Another distinguishing feature is that rat BM-derived stem cells, which we isolated previously, did not require leukemia inhibitory peptide for culture expansion (data not shown) (35), which has been suggested to be essential for murine MAPC cultures.

Recent studies have demonstrated an important role of cell fusion in stem cell plasticity. Both in vitro (25) and in vivo (26, 28) experiments using ES cells and/or BM-derived stem cells showed that cell fusion is responsible for a certain percentage of phenotypic changes observed following stem cell transplantation. Cell fusion occurs in normal mammalian development during the formation of osteoclasts (36) and myoblasts (37) or during tumor progression (38). Recent in vivo studies suggest that hepatocytes derived from cell fusion of HSCs and host hepatocytes can correct underlying metabolic disorders and that fused cells can undergo reduction division (26). The present in vitro data indicate that both fusion and transdifferentiation could be responsible for the phenotypic changes of hBMSCs to ECs, SMCs, and CMCs, and furthermore that the prevalence depends on cell type. Although no definitive studies were performed in vivo to quantify the contribution of cell fusion to phenotypic changes observed, the results of in vitro studies implied that both fusion and differentiation can play a role. Although some recent studies raised controversy regarding the transdifferentiation potential of HSCs (12, 13), another recent study still claimed this potential (39). More importantly, these studies were performed using specifically defined subpopulations of HSCs, while our studies have used an entirely different stem population derived from BM.

In the past, recovery of cardiac function following MI has been considered to be completely dependent on the integrity of the remaining noninfarcted portion of the LV. Following MI, the viable myocardial tissue bordering the infarct area can undergo hypertrophy to compensate for lost CMCs (40). However, replenishment of lost CMCs was thought to be impossible. Moreover, although neovascularization within the infarcted tissue appears to be an integral component of the remodeling process, under normal circumstances the capillary network cannot keep pace with tissue growth and is unable to support the greater demands of the hypertrophied but viable myocardium, which subsequently undergoes apoptosis and necrosis due to inadequate oxygenation and nutrient supply, leading to further deterioration of cardiac function (41). Thus far, no studies using human stem cells derived from BM have documented both therapeutic neovascularization and cardiomyogenesis following MI. Our experiments show that transplantation of a clonal adult human stem cell population can replenish both vascular networks and cardiac muscle, and they also reveal that the therapeutic effect consists of endogenous tissue repair (angiogenesis and endogenous cardiomyogenesis) as well as exogenous tissue regeneration (vasculogenesis and exogenous cardiomyogenesis). A key observation is that the rate of engraftment and cell survival was remarkably higher following hBMSC transplantation compared with TBMC transplantation. It seems highly probable that this prolonged interaction between host and transplanted hBMSCs, by promoting secretion of multiple paracrine factors and augmenting direct cell-to-cell contact, could lead to a significantly higher degree of endogenous cardiomyogenesis and angiogenesis as well as the differentiation of local stem cells (27, 42).

To induce angiogenesis and/or arteriogenesis, tight orchestration of monocytes/macrophages, ECs, and SMCs/pericytes is critical (22, 43). PDGF-B is prerequisite for the investment of stable vessels with pericytes (31). Given the complex structure of formed mature vessels with periendothelial matrix and pericytes/SMCs, a combination of various angiogenic growth factors may be advantageous (22, 43, 44). In addition to documenting direct vasculogenesis from transplanted stem cells, these studies suggest a potential additional benefit of hBMSC transplantation into ischemic myocardium, augmenting neovascularization by supplying various angiogenic cytokines (VEGF, angiopoietin-1 and -2, bFGF, HGF, PDGF-B).

Moreover, as IGF, VEGF, bFGF, and HGF are known to function as survival factors for the endangered CMCs (45, 46), these paracrine effects may be as important as the differentiation potential of stem cells for neovascularization.

Interestingly, our study demonstrated no functional improvement in unselected total BM–transplanted rats, which apparently differ from those of the previous studies using BM cells (47, 48). The discrepancy of therapeutic effects could result from the difference in animal models and the cells used. One study (47) used cultured BM cells in a pig model of chronic MI, and the other study (48) used mononuclear cells in porcine MI model. Our study used *unselected* BM cells in a large infarction model in rats. The size of infarction created is much smaller in pigs than in rats because pigs cannot tolerate large infarctions as a result of mechanical dysfunction and arrhythmia. In the large infarction we induced in rats, use of unselected BM cells may result in a failure of therapeutic effect because of an insufficient dose of therapeutic cells or by the inclusion of cells that may actually have a detrimental effect.

Since the loss of CMCs plays the most direct role in the development of heart failure, cardiomyogenesis has been the central aim of cardiac regenerative therapy using stem cells. Our results demonstrate direct differentiation of hBMSCs into CMCs, which we define as exogenous cardiomyogenesis. Our data also reveal significant endogenous cardiomyogenesis, i.e., generation of new CMCs from the host myocardium after hBMSC transplantation. Upregulation of cardiac transcription factors further supports cardiomyogenesis after hBMSC transplantation. This phenomenon of endogenous cardiomyogenesis after stem cell transplantation has not, to our knowledge, been previously reported. The recent discovery of cardiac progenitor or stem cells (27, 42) supports the possibility of stimulation of endogenous cardiac progenitor or stem cells by engrafted hBMSCs. Whether this effect is a general mechanism in other stem cell transplantation remains to be determined.

One issue that must be considered in the realm of transplantation of cells into the heart is the provocation of arrhythmia. In the present study, 14 of 15 rats survived in the hBMSC group, compared with 12 of 15 in both the TBMC and the PBS groups. Although we could not monitor the animals continuously for the occurrence of arrhythmias, repetitive echocardiography with electrocardiographic monitoring was performed, which did not reveal arrhythmias in any of the treatment groups. In this regard it is noteworthy that the arrhythmic events that have been reported thus far have occurred following skeletal myoblast transplantation (49), while no events have been reported following transplantation of BM or circulating cells. We think this may be the result of the fact that skeletal muscle and cardiac muscle cells depolarize and repolarize actively, while marrow-derived progenitors are passive. Nevertheless, caution is mandated in the early phases of all studies of intramyocardial cell transplantation.

Compared with the other human stem cells or progenitor cells, hBMSCs have certain potential advantages for regenerative therapy of cardiac diseases. Among the human stem cells shown to improve cardiac function are endothelial progenitor cells (14), $CD34^+$ cells (16), and angioblasts (15), which have been shown to promote neovascularization in vivo. Human ES cells have demonstrated the potential to differentiate into CMCs in vitro (50), but recent human ES cell transplantation into murine ischemic hearts has been shown to result in teratoma formation. Human MSCs have been shown to transdifferentiate into CMCs. However, the number of transdifferentiated cells was small, transdifferentiation into ECs and SMCs was not demonstrated, and functional data in vivo were not generated (20). In contrast, hBMSCs have the required multipotency in vitro and in vivo to regenerate damaged myocardium, are culture-expandable, and disclose the functional capability for therapeutic application. Finally, considering the scope of multipotency of the hBMSCs and the robust nature of engraftment, it is possible that the use of hBMSCs may extend to a therapeutic arena including other degenerative or inherited diseases.

Coronary artery disease accounts for 50% of all cardiovascular deaths and nearly 40% of the incidence of heart failure (1). The current findings have provided evidence that hBMSC transplantation could have relevant implications for the treatment of human disease. We have been able to demonstrate here, for the first time to our knowledge, that *adult human* stem cells can augment both therapeutic neovascularization and cardiomyogenesis, thereby enhancing functional and anatomic regeneration after MI. This new form of cardiac repair may improve the immediate and long-term outcome of ischemic heart disease and may therefore merit clinical investigation in patients with ischemic heart disease.

Methods

Isolation and culture of BM-derived stem cells. Fresh unprocessed human BM from young male donors was purchased from Cambrex Corp. BM was centrifuged at 350 *g* for 10 minutes to obtain cell pellets, which then were resuspended in 25 ml of Dulbecco's PBS (DPBS) containing 0.5 M EDTA. After centrifugation at 350 *g* for 7 minutes, the cells were resuspended in 5 ml DPBS containing 0.5 M EDTA and 20 ml of NH_4Cl for induction of hemolysis. After centrifugation and washing with DPBS containing 0.5 M EDTA, cells were filtered through a 40-μm nylon filter and plated in wells of 6-well plates that had been coated with fibronectin (100 μg/ml). The cells were grown at a density of 5×10^6 per square centimeter in complete DMEM with low (1 g) glucose containing 17% of FBS (lot selected for promoting expansion of marrow cells; Cambrex Corp.), 100 U/ml penicillin, and 100 μg/ml streptomycin and 2 mM glutamate at 37°C and 5% CO_2. Once the attached cells began to form colonies (4–6 days), the medium was replaced and the adherent cells were grown to 60% confluence. Next, the cells were reseeded in complete medium into 25-cm^2 tissue culture flasks at a density of 1×10^4 cells per square centimeter. After the cells were 60% confluent, they were serially reseeded into 75-cm^2 and 175-cm^2 flasks at the same density. After at least 2 passages of cultures in 175-cm^2 flasks, cells were labeled with CellTracker CM-DiI (DiI; Invitrogen Corp.), plated into the wells of a 96-well plate at a density of 0.5 cell per well by limiting-dilution method, and cultured with conditioned media, which were collected prior to limiting dilution, stored in –80°C, and filtered through a 0.22-μm sterile filter (Fisher Scientific International Inc.). After the exclusion of wells containing more than 1 cell under fluorescent microscopy, the clones derived from a single cell were further cultured (Figure 1, A and B). When these cells were grown to 40–50% confluence, cells from 1 well were reseeded into 1 well of a 6-well plate and thereafter serially reseeded in 25-cm^2, 75-cm^2, and 175-cm^2 flasks when cells reached 30% confluence. When the cells reached a density of 4×10^3 to 8×10^3 cells per square centimeter in 175-cm^2 flasks, they were replated at 1:40 to 1:10 dilution; this process was repeated through 140 PDs. All reseeding was performed in triplicate, and the fastest-growing clone was selected through 50–60 PDs.

Fluorescence-activated cell sorting and DNA ploidy analysis. Fluorescence-activated cell sorting (FACS; BD Biosciences) analysis of hBMSCs was performed on cultured hBMSCs. Specimens were selected from at least 3 different populations of clonal lines, and for clonal lines, 2 sets of cells at 5 PDs and 120 PDs were used. The procedure of FACS staining was described previously (51). In brief, a total of 2×10^5 cultured cells were resuspended with 200 μl of

Dulbecco's PBS (Cambrex Corp.) containing 10% FBS and 0.01% NaN_3 and incubated for 30 minutes at 4°C with directly PE- or FITC-conjugated mAbs or nonconjugated Abs followed by a FITC-conjugated rabbit antimouse IgG (Jackson ImmunoResearch Laboratories Inc.). Proper isotype-identical Igs served as controls. After staining, the cells were fixed in 2% paraformaldehyde, and quantitative FACS was performed on a FACStar flow cytometer (BD). Abs used for FACS analysis were FITC- or PE-conjugated Abs against CD4, CD8, CD11b (Mac-1), CD13, CD14, CD15, CD29, CD30, CD31, CD34, CD44, CD49e, CD71, CD73, CD90 (Thy1), CD117 (c-kit), CD146, CD166, HLA-DR, HLA-ABC, β_2-microglobulin (all from BD), CD133 (AC133; Miltenyi Biotec Inc.), and CD105 (endoglin; Ancell Corp.), unconjugated Abs against Oct4 (Santa Cruz Biotechnology Inc.), and isotype control Igs (BD). For comparison, human mesenchymal stem cells (PT-2501) and media (PT-3001) were purchased from Cambrex Corp. and used for FACS.

DNA contents per cell were determined by pretreatment of cells with ribonuclease (100 μg/ml), staining with propidium iodide (50 μg/ml), and subsequent FACS analysis.

Telomere length and telomerase assay. We used a TeloTAGGG telomere length assay kit (Roche Diagnostics Corp.) for determination of mean telomere length of hBMSCs at 5 PDs and 120 PDs from 3 different clones. Briefly, after isolation (1 μg) and digestion of genomic DNA, DNA fragments were separated by gel electrophoresis and transferred to a nylon membrane by Southern blotting. The blotted DNA fragments were hybridized to a digoxigenin-labeled probe specific for TRF and incubated with a digoxigenin-specific Ab covalently coupled to alkaline phosphate. Finally, the immobilized telomere probe was visualized by alkaline phosphatase metabolizing CDP-Star, a highly sensitive chemiluminescence substrate. The average TRF length was determined by comparison of the signals relative to a molecular weight standard. We also performed telomeric repeat amplification protocol (TRAP) assay to detect telomerase activity in hBMSCs with a TeloTAGGG telomerase PCR kit (Roche Diagnostics Corp.).

In vitro differentiation of hBMSCs. All of the following in vitro studies were performed using 3 different clonal hBMSCs of 5 and 90 PDs. To induce differentiation into ECs, hBMSCs were replated at 5×10^4 cells per square centimeter in DMEM or EBM-2 (Cambrex Corp.) with 2% FBS, 10^{-8} dexamethasone, and 10 ng/ml VEGF (R&D Systems Inc.) in glass chamber slides coated with either 0.1% gelatin or fibronectin, and cultured for up to 14 days. To induce differentiation into SMC phenotypes, hBMSCs were replated at 1×10^5 cells per square centimeter in noncoated or fibronectin-coated culture dishes in 1–2% DMEM or EBM-2 supplemented with PDGF-BB (50 ng/ml; R&D Systems Inc.) (22) and cultured for 14 days. To induce neural lineage differentiation, hBMSCs were plated at 4×10^4 per square centimeter on BioCoat poly-L-ornithine/laminin–coated dishes (BD) or plastic dishes with 100 ng/ml bFGF, 20 ng/ml EGF, and B27 supplement in DMEM/F12 (3, 4) and cultured for up to 14 days. To induce endodermal lineage differentiation, hBMSCs were plated at 3×10^4 to 4×10^4 cells per square centimeter on 1% Matrigel (BD) in 2% FBS, supplemented with 10^{-8} dexamethasone, 25 ng/ml HGF, and 10 ng/ml FGF-4, and cultured for 7 days; thereafter, either 10 mg/ml DMSO or 0.5 mM sodium butyrate was added and cultured for 7 more days (21, 23). To induce CMC differentiation of the hBMSCs, hBMSCs were cocultured with freshly isolated NRCMs. Primary NRCMs from F344 rats were isolated as described previously (52) and plated at 2×10^5 cells per square centimeter. DiI-labeled hBMSCs were added to the NRCM culture plates at a 1:4 ratio in DMEM containing 10% FCS and cultured for up to 14 days.

In vitro fusion studies. RAECs were cultured in EBM-2 containing EGM-2 MV SingleQuots (Cambrex Corp.). RVSMCs were cultured in DMEM with 1 g/l glucose containing 15% FBS, 2 mM L-glutamine, and antibiotics. NRCMs were isolated and cultured as described above. When the cells reached 50–60% confluence (within 3 days), cells were stained with 25 μM of Vybrant CFDA-SE cell tracer kit (Invitrogen Corp.) according to the manufacturer's instructions. Cells labeled with CFDA-SE appeared green under fluorescent microscopy. Two days later, DiI-labeled hBMSCs (red fluorescence) were added to culture plates of RAECs, RVSMCs, or NRCMs at a 1:4 ratio and cultured for 7 days. Media were changed every 2–4 days. To determine the prevalence of fusion and differentiation, 5,000 cells were counted per coculture from 3 different experiments. To verify these results, we performed coculture experiments under the same conditions using hBMSCs lentivirally transfected with GFP and NRCMs, RAECs, and RVSMCs adenovirally transfected with LacZ (53).

Abs used for IF cytochemistry. For immunocytochemistry, cells were fixed in 4% cold paraformaldehyde for 7 minutes and washed with PBS twice. As EC markers, we used Abs against vWFa (goat polyclonal Ab [pAb], 1:400), Flk1 (mouse mAb, 1:300; Santa Cruz Biotechnology Inc.), VE-cadherin (mouse mAb, 1:100; BD), CD31 (mouse mAb, 1:100; BD), ULEX (1:200; Vector Laboratories Inc.), and ILB4 (1:200; Vector Laboratories Inc.). As SMC markers, we used Abs against α-SMA (mouse mAb, 1:300; Sigma-Aldrich) and calponin (mouse mAb, 1:250; DAKO Corp.). As neural lineage markers, we used Abs against NF200 (mouse mAb, 1:400; Sigma-Aldrich), β-tubulin III isoform (mouse mAb, 1:100; Sigma-Aldrich), GalC (rabbit pAb, 1:100; Sigma-Aldrich), and GFAP (goat pAb, 1:200; Santa Cruz Biotechnology Inc.). As endodermal (hepatocytic or other epithelial) lineage markers, we used CK18 (mouse mAb, 1:300; Sigma-Aldrich), α-fetoprotein (goat pAb, 1:200; Santa Cruz Biotechnology Inc.), albumin (mouse mAb, 1:400; Sigma-Aldrich), HNF3β (goat pAb, 1:100; Santa Cruz Biotechnology Inc.), and HNF1α (rabbit pAb, 1:200; Santa Cruz Biotechnology Inc.). As CMC markers, we used Abs against cTnI (2 forms: mouse mAb and rabbit pAb, 1:100; Chemicon International Inc.), ventricular α-MHC (mouse mAb, 1:100; Chemicon International Inc.), α-sarcomeric actinin (clone EA-53, mouse mAb, 1:200; Sigma-Aldrich), and ANP (rabbit pAb, 1:100; Chemicon International Inc.). Control mouse, rabbit, and goat Igs were from Sigma-Aldrich. Secondary anti-mouse, -rabbit, and -goat Igs (AMCA, 1:150; FITC or Cy2, 1:200; Cy3, 1:200) were from Jackson ImmunoResearch Laboratories Inc.

Study design of in vivo experiments. All animal procedures were approved by the Institutional Animal Care and Use Committee of Caritas St. Elizabeth's Medical Center. Six- to 7-week-old female nude rats (Hsd:RH-*rnu* rats; Harlan) underwent surgery to induce acute MI as described previously in our laboratory (14, 16). Briefly, following left thoracotomy and incision of the pericardium under artificial ventilation (Harvard Small Animal Ventilator model 683; Harvard Apparatus Co.), the left anterior descending coronary artery was ligated near its origin with a 6-0 prolene suture (Ethicon Inc.). Immediately after surgery, the rats were randomly assigned to 1 of 3 treatment groups (n = 15 per group) and received 8×10^5 hBMSCs, 8×10^5 human fresh TBMCs, or PBS in a total volume of 200 μl via intramyocardial injection at 5 sites in the peri-infarct area (basal anterior, mid-anterior, mid-lateral, apical anterior, and apical lateral). The preparation of TBMCs was identical to that of hBMSCs before culture. hBMSCs and TBMCs were labeled with the carbocyanine dye CM-DiI (DiI; 1.5 μg/ml; Invitrogen Corp.) before the cell transplantation as described previously (14, 51). The rats underwent echocardiography 3 days and 4 weeks after surgery and invasive hemodynamic measurements 4 weeks after surgery. After the surgery, separate rats (n = 4 per group) were implanted underneath the back skin with miniosmotic pumps (model 2ML4, ALZET; DURECT Corp.) that infused 1.25 mg BrdU per day (Sigma-Aldrich) (dissolved in a 1:1 [vol/vol] mixture of dimethyl sulfoxide and 0.154 M NaCl) and were sacrificed at 4 weeks (54). For apoptosis assay (n = 5 per group) and molecular studies (n = 3 per group), other rats were similarly operated on and sacrificed 1 week and 4 weeks after surgery, respectively. Rats were sacrificed with saline perfusion into the aorta. At necropsy, the hearts were sliced into 3 transverse sections from apex to base, either fixed with 4% paraformaldehyde or methanol or frozen in OCT compound, and sectioned with 5 μm thickness.

Cardiac function measurements. Transthoracic echocardiography was performed with a 6.0- to 15.0-MHz ultraband linear transducer connected to SONOS 5500 (Agilent Technologies Inc.) as described previously (16). LVEDD, LVESD, and fractional shortening were measured. All measurements represent the mean of at least 3 consecutive cardiac cycles. WMSI was used to evaluate regional wall motion abnormality (55). LV wall motion analysis is based on grading of contractility of an individual segment. In this scoring system, a higher score indicates more severe wall motion abnormality (1, normal; 2, hypokinesis; 3, akinesis; 4, dyskinesis; 5, aneurysm). A WMSI is derived by division of the sum of wall motion scores by the number of visualized segments and represents the extent of regional wall motion abnormalities. To measure hemodynamic variables, a 1.4 French high-fidelity pressure transducer (Mikro-Tip catheter; Millar Instruments Inc.) was introduced into the LV via the right carotid artery. After the hemodynamics stabilized, LV systolic pressure, LV end-diastolic pressure (LVEDP), +dP/dt, and –dP/dt were recorded using a polygraph (model 7P; Grass Instruments).

IF histochemistry of cardiac tissues and TUNEL assay. OCT-embedded frozen sections were fixed in 4% paraformaldehyde for 7 minutes and used for immunohistochemical analysis. For identification of ECs, biotinylated ILB4 (1:200; Vector Laboratories Inc.) was used as a primary Ab and was followed by streptavidin-FITC (1:100) (14). SMCs were identified by mouse α-SMA Ab (1:300) followed by FITC-conjugated goat antimouse IgG. CMCs were identified by Abs against cTnI and ANP followed by FITC-conjugated goat antirabbit IgG. BrdU was detected with the sheep anti-BrdU Ab (1:50; BIODESIGN International) followed by streptavidin-FITC (1:100; Vector Laboratories Inc.). BrdU-positive cells were counted in the peri-infarct area, where the scar tissue constitutes less than 20% of the visual field (×200 magnification). Nuclear counterstaining was performed with DAPI. Ki-67 staining was performed to determine the instantaneous proliferative fraction with samples obtained at 1 week as described previously (56).

In situ labeling of fragmented DNA was performed with the TUNEL method with the use of an in situ cell detection kit (Roche Diagnostics Corp.) according to the manufacturer's instructions. TUNEL assay was conducted on myocardial sections obtained at 1 week (n = 4 per group). Briefly, sections were treated with 20 μg of proteinase K, washed, and then incubated in a solution of terminal deoxynucleotidyl transferase (TdT) with fluorescein dUTP mixture. The sections were then counterstained with DAPI for localization of nuclei. To determine the proportion of apoptotic nuclei within CMCs or ECs, tissue was counterstained with a mAb against α-sarcomeric actinin or ILB4. Double immunohistochemistry with Ab against activated caspase-3 (1:250; Promega Corp.) and Ab against α-sarcomeric actinin was performed to confirm myocardial apoptosis. Tissue sections were examined microscopically under ×200 magnification, and a total of 8 random visual fields (total of approximately 10,000 nuclei) in the infarct and peri-infarct area were examined. The percentage of apoptotic cells was termed the apoptotic index.

FISH of human Y chromosome. FISH was performed on 4% paraformaldehyde–fixed tissue sections according to the manufacturer's instructions. We used a CEP Y DNA probe (DYZ1 locus; Vysis Inc.), a DNA probe that is labeled with SpectrumOrange (a red fluorescence dye; Vysis Inc.) and is specific for Satellite III at the Yq12 region of human Y chromosome (57). Briefly, after deparaffinization and rehydration, sections attached on slides were treated with 0.2N HCl for 20 minutes and washed in 2× SSC (0.3 M NaCl, 30 mM sodium citrate in normal saline). Then the glass jar containing sections was heated in an 80°C water bath for 20 minutes. After washing with 2× SSC, sections were treated with proteinase K in Tris-EDTA-NaCl (TEN) buffer for 10 minutes at 37°C and then fixed with 4% formaldehyde followed by serial ethanol dehydration. Next, after application of the probe to sections, the probe and target DNA were denatured simultaneously for 10 minutes at 90°C, and the sections were incubated overnight at 42°C in a humidified chamber. The sections were washed in 2× SSC/50% formamide for 5 minutes at 42°C twice. Finally, the sections were counterstained with DAPI, covered with a mounting medium, and examined under fluorescent microscopy. FISH was followed by immunohistochemistry using ILB4, anti–α-sarcomeric actinin, or anti–α-SMA Ab to detect differentiation of hBMSCs into CMC, EC, and SMC lineages, respectively.

Western blot and RT-PCR analysis. Western blot was performed as described previously (56). Briefly, after samples were homogenized in lysis buffer, protein extracts (100 μg per sample) were separated using SDS-PAGE (Bio-Rad Laboratories) and electrotransferred onto PVDF membranes (Amersham Pharmacia Biotech Inc.). Samples were probed with rabbit pAbs against VEGF (1:500), HGF (1:500), and bFGF (1:500; all from Santa Cruz Biotechnology Inc.) overnight at 4°C. Equal protein loading was confirmed by reprobing of the membranes with a mouse mAb to α-tubulin (1:1,000; Calbiochem Immunochemicals). RT-PCR was performed as described previously (56). Total RNA was extracted from cultured cells or from hearts using an RNAqueous kit (Ambion Inc.) according to the manufacturer's instructions. One microgram of total RNA was reverse-transcribed using random hexamer and Moloney murine leukemia virus reverse transcriptase (SuperScript II kit; Roche Diagnostics Corp.). The RT product was subjected to PCR using Advantage cDNA polymerase mix (BD Biosciences — Clontech) or Taq polymerase (Roche Diagnostics Corp.). To prove the absence of the expression of certain genes, we used 40 cycles for each gene expression. For semiquantitative RT-PCR, the quantification of mRNA expression of each gene was calculated based on the GAPDH expression. The PCR primers used are described in Supplemental Table 1. RT-PCR products were analyzed by 1.5% agarose gel electrophoresis with a 100-bp ladder (Invitrogen Corp.) and quantified with the UV imager Eagle Eye II (Stratagene).

Analysis of cardiac histology and morphometry. Capillary density and CMC density were counted after the staining of samples 4 weeks after transplantation with mAb against CD31 and H&E, respectively, as described previously (14, 16). A total of 8 visual fields where a cross section of capillaries and CMCs was clearly visible were randomly selected in the infarct and peri-infarct area, and the number of capillaries or CMCs was counted under ×200 magnification (n = 6 per group). To determine the fibrosis area, the average ratio of fibrosis area per LV area was measured for all histologic sections after staining with Masson's trichrome (Sigma-Aldrich) as described previously (14).

Statistical analysis. Statistical analysis was performed by an unpaired Student's t test for comparisons between 2 groups and ANOVA followed by Scheffe's post hoc or χ^2 test for comparisons of more than 2 groups. P less than 0.05 is considered statistically significant.

Acknowledgments

This study was supported in part by NIH grants HL53354, HL60911, HL63414, HL63695, and HL-66957 (to D.W. Losordo) and an American Heart Association National Scientist Development Grant (to Y.-S. Yoon). The authors thank Mickey Neely for her assistance in the preparation of the manuscript.

Received for publication June 2, 2004, and accepted in revised form December 7, 2004.

Address correspondence to: Douglas W. Losordo or Young-sup Yoon, Cardiovascular Research, St. Elizabeth's Medical Center, 736 Cambridge Street, Boston, Massachusetts 02135, USA. Phone: (617) 789-3346; Fax: (617) 779-6362; E-mail: douglas.losordo@tufts.edu (Douglas W. Losordo). Phone: (617) 562-7523; Fax: (617) 562-7506; E-mail: young.yoon@tufts.edu (Young-sup Yoon).

1. Braunwald, E., and Bristow, M.R. 2000. Congestive heart failure: fifty years of progress. *Circulation.* **102**:IV14–IV23.
2. Pfeffer, M.A. 1995. Left ventricular remodeling after acute myocardial infarction. *Annu. Rev. Med.* **46**:455–466.
3. Brazelton, T.R., Rossi, F.M., Keshet, G.I., and Blau, H.M. 2000. From marrow to brain: expression of neuronal phenotypes in adult mice. *Science.* **290**:1775–1779.
4. Mezey, E., Chandross, K.J., Harta, G., Maki, R.A., and McKercher, S.R. 2000. Turning blood into brain: cells bearing neuronal antigens generated in vivo from bone marrow. *Science.* **290**:1779–1782.
5. Ferrari, G., et al. 1998. Muscle regeneration by bone marrow-derived myogenic progenitors. *Science.* **279**:1528–1530.
6. Orlic, D., et al. 2001. Bone marrow cells regenerate infarcted myocardium. *Nature.* **401**:701–705.
7. Jackson, K.A., et al. 2001. Regeneration of ischemic cardiac muscle and vascular endothelium by adult stem cells. *J. Clin. Invest.* **107**:1395–1402.
8. Asahara, T., et al. 1999. Bone marrow origin of endothelial progenitor cells responsible for postnatal vasculogenesis in physiological and pathological neovascularization. *Circ. Res.* **85**:221–228.
9. Lagasse, E., et al. 2000. Purified hematopoietic stem cells can differentiate into hepatocytes in vivo. *Nat. Med.* **6**:1229–1234.
10. Krause, D.S., et al. 2001. Multi-organ, multi-lineage engraftment by a single bone marrow-derived stem cell. *Cell.* **105**:369–377.
11. Jiang, Y., et al. 2002. Pluripotency of mesenchymal stem cells derived from adult marrow. *Nature.* **418**:41–49.
12. Balsam, L.B., et al. 2004. Haematopoietic stem cells adopt mature haematopoietic fates in ischaemic myocardium. *Nature.* **428**:668–673.
13. Murry, C.E., et al. 2004. Haematopoietic stem cells do not transdifferentiate into cardiac myocytes in myocardial infarcts. *Nature.* **428**:664–668.
14. Kawamoto, A., et al. 2001. Therapeutic potential of ex vivo expanded endothelial progenitor cells for myocardial ischemia. *Circulation.* **103**:634–637.
15. Kocher, A.A., et al. 2001. Neovascularization of ischemic myocardium by human bone-marrow-derived angioblasts prevents cardiomyocyte apoptosis, reduces remodeling and improves cardiac function. *Nat. Med.* **7**:430–436.
16. Kawamoto, A., et al. 2003. Intramyocardial transplantation of autologous endothelial progenitor cells for therapeutic neovascularization of myocardial ischemia. *Circulation.* **107**:461–468.
17. Prockop, D.J. 1997. Marrow stromal cells as stem cells for nonhematopoietic tissues. *Science.* **276**:71–74.
18. Pittenger, M.F., et al. 1999. Multilineage potential of adult human mesenchymal stem cells. *Science.* **284**:143–147.
19. Makino, S., et al. 1999. Cardiomyocytes can be generated from marrow stromal cells in vitro. *J. Clin. Invest.* **103**:697–705.
20. Toma, C., Pittenger, M.F., Cahill, K.S., Byrne, B.J., and Kessler, P.D. 2002. Human mesenchymal stem cells differentiate to a cardiomyocyte phenotype in the adult murine heart. *Circulation.* **105**:93–98.
21. Schwartz, R.E., et al. 2002. Multipotent adult progenitor cells from bone marrow differentiate into functional hepatocyte-like cells. *J. Clin. Invest.* **109**:1291–1302. doi:10.1172/JCI200215182.
22. Yamashita, J., et al. 2000. Flk1-positive cells derived from embryonic stem cells serve as vascular progenitors. *Nature.* **408**:92–96.
23. Oh, S.H., et al. 2000. Hepatocyte growth factor induces differentiation of adult rat bone marrow cells into a hepatocyte lineage in vitro. *Biochem. Biophys. Res. Commun.* **279**:500–504.
24. Srivastava, D., and Olson, E.N. 2000. A genetic blueprint for cardiac development. *Nature.* **407**:221–226.
25. Terada, N., et al. 2002. Bone marrow cells adopt the phenotype of other cells by spontaneous cell fusion. *Nature.* **416**:542–545.
26. Wang, X., et al. 2003. Cell fusion is the principal source of bone-marrow-derived hepatocytes. *Nature.* **422**:897–901.
27. Oh, H., et al. 2003. Cardiac progenitor cells from adult myocardium: homing, differentiation, and fusion after infarction. *Proc. Natl. Acad. Sci. U. S. A.* **100**:12313–12318.
28. Alvarez-Dolado, M., et al. 2003. Fusion of bone-marrow-derived cells with Purkinje neurons, cardiomyocytes and hepatocytes. *Nature.* **425**:968–973.
29. Bussolino, F., et al. 1992. Hepatocyte growth factor is a potent angiogenic factor which stimulates endothelial cell mobility and growth. *J. Cell Biol.* **119**:629–641.
30. Asahara, T., et al. 1998. Tie2 receptor ligands, angiopoietin-1 and angiopoietin-2, modulate VEGF-induced postnatal neovascularization. *Circ. Res.* **83**:233–240.
31. Folkman, J., and D'Amore, P.A. 1996. Blood vessel formation: what is its molecular basis? *Cell.* **87**:1153–1155.
32. Yamaguchi, J., et al. 2003. Stromal cell-derived factor-1 effects on ex vivo expanded endothelial progenitor cell recruitment for ischemic neovascularization. *Circulation.* **107**:1322–1328.
33. Barry, F.P., Boynton, R.E., Haynesworth, S., Murphy, J.M., and Zaia, J. 1999. The monoclonal antibody SH-2, raised against human mesenchymal stem cells, recognizes an epitope on endoglin (CD105). *Biochem. Biophys. Res. Commun.* **265**:134–139.
34. Barry, F., Boynton, R., Murphy, M., Haynesworth, S., and Zaia, J. 2001. The SH-3 and SH-4 antibodies recognize distinct epitopes on CD73 from human mesenchymal stem cells. *Biochem. Biophys. Res. Commun.* **289**:519–524.
35. Yoon, Y.-S., et al. 2002. Clonally expanded bone marrow (BM) derived stem cells differentiate into multiple lineages in vitro and can attenuate myocardial dysfunction post myocardial infarction (MI) [abstract]. *Circulation.* **106**(Suppl. II):11.
36. Vignery, A. 2000. Osteoclasts and giant cells: macrophage-macrophage fusion mechanism. *Int. J. Exp. Pathol.* **81**:291–304.
37. Mintz, B., and Baker, W.W. 1967. Normal mammalian muscle differentiation and gene control of isocitrate dehydrogenase synthesis. *Proc. Natl. Acad. Sci. U. S. A.* **58**:592–598.
38. Kerbel, R.S., Lagarde, A.E., Dennis, J.W., and Donaghue, T.P. 1983. Spontaneous fusion in vivo between normal host and tumor cells: possible contribution to tumor progression and metastasis studied with a lectin-resistant mutant tumor. *Mol. Cell. Biol.* **3**:523–538.
39. Bailey, A.S., et al. 2004. Transplanted adult hematopoietic stems cells differentiate into functional endothelial cells. *Blood.* **103**:13–19.
40. Olivetti, G., Capasso, J.M., Meggs, L.G., Sonnenblick, E.H., and Anversa, P. 1991. Cellular basis of chronic ventricular remodeling after myocardial infarction in rats. *Circ. Res.* **68**:856–869.
41. Cheng, W., et al. 1996. Programmed myocyte cell death affects the viable myocardium after infarction in rats. *Exp. Cell Res.* **226**:316–327.
42. Beltrami, A.P., et al. 2003. Adult cardiac stem cells are multipotent and support myocardial regeneration. *Cell.* **114**:763–776.
43. Carmeliet, P. 2000. Mechanisms of angiogenesis and arteriogenesis. *Nat. Med.* **6**:389–395.
44. Ferrara, N., and Alitalo, K. 1999. Clinical applications of angiogenic growth factors and their inhibitors. *Nat. Med.* **5**:1359–1364.
45. Giordano, F.J., et al. 2001. A cardiac myocyte vascular endothelial growth factor paracrine pathway is required to maintain cardiac function. *Proc. Natl. Acad. Sci. U. S. A.* **98**:5780–5785.
46. Kitta, K., et al. 2003. Hepatocyte growth factor induces GATA-4 phosphorylation and cell survival in cardiac muscle cells. *J. Biol. Chem.* **278**:4705–4712.
47. Fuchs, S., et al. 2001. Transendocardial delivery of autologous bone marrow enhances collateral perfusion and regional function in pigs with chronic experimental myocardial ischemia. *J. Am. Coll. Cardiol.* **37**:1726–1732.
48. Kamihata, H., et al. 2001. Implantation of bone marrow mononuclear cells into ischemic myocardium enhances collateral perfusion and regional function via side supply of angioblasts, angiogenic ligands, and cytokines. *Circulation.* **104**:1046–1052.
49. Menasche, P., et al. 2003. Autologous skeletal myoblast transplantation for severe postinfarction left ventricular dysfunction. *J. Am. Coll. Cardiol.* **41**:1078–1083.
50. Kehat, I., et al. 2001. Human embryonic stem cells can differentiate into myocytes with structural and functional properties of cardiomyocytes. *J. Clin. Invest.* **108**:407–414. doi:10.1172/JCI200112131.
51. Kalka, C., et al. 2000. Transplantation of ex vivo expanded endothelial progenitor cells for therapeutic neovascularization. *Proc. Natl. Acad. Sci. U. S. A.* **97**:3422–3427.
52. De Luca, A., et al. 2000. Characterization of caveolae from rat heart: localization of postreceptor signal transduction molecules and their rearrangement after norepinephrine stimulation. *J. Cell. Biochem.* **77**:529–539.
53. Lois, C., Hong, E.J., Pease, S., Brown, E.J., and Baltimore, D. 2002. Germline transmission and tissue-specific expression of transgenes delivered by lentiviral vectors. *Science.* **295**:868–872.
54. McEwan, P.E., Gray, G.A., Sherry, L., Webb, D.J., and Kenyon, C.J. 1998. Differential effects of angiotensin II on cardiac cell proliferation and intramyocardial perivascular fibrosis in vivo. *Circulation.* **98**:2765–2773.
55. Oh, J.K., Seward, J.B., and Tajik, A.J. 1999. Assessment of ventricular systolic function. In *The echo manual*. Lippincott-Raven. Philadelphia, Pennsylvania, USA. 37–43.
56. Yoon, Y.-S., et al. 2003. VEGF-C gene therapy augments postnatal lymphangiogenesis and ameliorates secondary lymphedema. *J. Clin. Invest.* **111**:717–725. doi:10.1172/JCI200315830.
57. Johnson, K.L., Zhen, D.K., and Bianchi, D.W. 2000. The use of fluorescence in situ hybridization (FISH) on paraffin-embedded tissue sections for the study of microchimerism. *Biotechniques.* **29**:1220–1224.